Author(s): Puska, M. J. & Nieminen, Risto M.

Title: Atoms embedded in an electron gas: Beyond the local-density approximation

Year: 1991

Version: Final published version

Please cite the original version:

Puska, M. J. & Nieminen, Risto M. 1991. Atoms embedded in an electron gas: Beyond the local-density approximation. Physical Review B. Volume 43, Issue 15. 12221-12233. ISSN 1550-235X (electronic). DOI: 10.1103/physrevb.43.12221.

Atoms embedded in an electron gas: Beyond the local-density approximation

M. J. Puska and R. M. Nieminen
Laboratory of Physics, Helsinki University of Technology, 02150 Espoo, Finland
(Received 7 May 1990)

The chemical-binding properties of atoms belonging to the first three rows of the Periodic Table are studied within the atom-in-jellium model. The electronic structures are solved self-consistently using the density-functional theory. The extraction of the binding properties is carried out in the framework of the effective-medium theory. The emphasis is put on the systematic investigation of the trends along the $2p$, $3p$, and $3d$ series and on the effects due to different types of approximations for electron exchange and correlation. More specifically, in addition to the popular local-density approximation, the self-interaction-correction scheme and the generalized-gradient approximation are employed. The results provide insight into why the local-density approximation for solids (molecules or chemisorption systems) overestimates the cohesive (binding) energies but gives the lattice constants (bond lengths) and bulk moduli (vibration frequencies) rather well. The results obtained are also important because they give the basic parameters for the effective-medium theory, which is a versatile approximative method for calculating total energies of systems with many interacting atoms.

I. INTRODUCTION

The density-functional theory introduced about a quarter of century ago by Hohenberg, Kohn, and Sham has been one of the success stories in theoretical solid-state physics.[1-3] The theory gives an exact recipe how the ground-state structure of a system of many interacting electrons can be solved as a problem of noninteracting particles and how the total energy of the ground state is calculable as a functional of the electron density. In practice, however, one has to make one approximation: the exchange-correlation part of the total-energy functional is not known exactly. By far the most popular way to proceed is to use the local-density approximation (LDA), in which the local exchange-correlation energy density and potential at a given point depend only on the electron density at that point. For these local quantities the results for the homogeneous electron gas are used. The LDA is very simple but has turned out to be very successful in describing various electronic properties of single atoms, molecules, and solids. The literature reporting on applications using density-functional theory within the LDA for predicting and/or understanding several types of properties of different systems is enormous.

The nature of the LDA itself has also been studied rather thoroughly, and, e.g., its success in also describing systems in which the electron density varies considerably is well understood.[4] The deficiencies of the LDA have also been studied carefully.[1] In the case of free atoms the most prominent shortcomings of the LDA are the instability of the negative ions and the too diffuse electron densities. These two errors reflect the wrong long-distance behavior of the one-electron potential in the LDA, and this behavior is in turn caused by the electron self-interaction effects inherent in the LDA. Moreover, the LDA predicts too high total energies for atoms. The errors in total energies are to a considerable extent canceled when calculating quantities related to energy differences. However, the ionization energies obtained are systematically somewhat too high and the s-p and s-d transfer energies too low.

In the case of solids, the perhaps most famous shortage is that density-functional theory within the LDA predicts for semiconductors and insulators band gaps which are too small, typically by about 50%. This property is traced back besides the LDA itself also to a discontinuity in the exchange-correlation potential as the number of electrons in the system changes.[5,6]

The important deficiency of the LDA connected with the description of formation of condensed systems of many atoms (molecules or solids) from free atoms is that the LDA predicts systematically too large binding energies. The binding energy in these cases is defined as the difference between the density-functional total energy of the compound system and that of the free atoms. It has been speculated[7] that the overbinding tendency is a general feature of the LDA, and the comparison of theory-experiment discrepancies for binding energies of dimers and cohesive energies of the corresponding solids supports this view. The discrepancies may be quite remarkable: in the case of diatomic molecules formed by the second row atoms of the Periodic Table the error reaches a value of ~ 2 eV for oxygen. On the other hand, the bond lengths and vibrational frequencies or bulk moduli are generally well predicted by the LDA. In the present work, while studying the deficiencies of the LDA we will limit ourselves to these binding or cohesive properties.

There exist several attempts and suggestions to go beyond the LDA. The gradient of the electron density is included, besides the local density, in the exchange-correlation energy functional, for example, in the generalized gradient approximation (GGA) introduced by Per-

dew and Wang Yue.[8] The average-density[9] (AD) and weighted-density[10] (WD) schemes are based on approximating the exact integral equation for the exchange-correlation hole. Furthermore, the exchange-correlation energy has been expressed as a wave-vector expansion, which has resulted in a general method by Langreth and Mehl,[11] also expressed as a gradient expansion. In the self-interaction correction (SIC) method by Perdew and Zunger[12] the interaction of a localized electron with itself in LDA is forced to vanish, which leads to a method with orbital-dependent effective one-electron potentials. However, none of these and other suggested methods has achieved such a widespread usage as the LDA. This is because usually a certain "beyond-LDA" method is able to improve the description some properties compared to the LDA, but a general improvement of all properties in different kinds of systems does not result. For example, in the case of free atoms the SIC gives more compact electron structures than the LDA and is able to predict the stability (electron affinity) of negative ions rather well,[12] but no systematic improvement on the LDA results for ionization and transfer energies.[13]

For the specific problem of the overbinding in the LDA, which we have mainly studied in this work, there are a few previous investigations. These are mainly concerned with the dimers formed by the second-row elements. Gunnarsson and Jones[14] concluded that the discrepancy between the experimental and the LDA values for the binding energy reflects the fact that the LDA cannot properly describe the nodal structure of molecular orbitals between the atoms. Significant improvement of the dissociation energies has been found in calculations using gradient corrections.[15,16] Moreover, Kutzler and Painter[16] showed that the nonspherical treatment of free atoms in calculations using nonlocal exchange-correlation functionals lowers the free-atom energies and thereby further lowers the dimer dissociation energies.

We will begin the presentation of the results of this work by demonstrating that the trends of atomic binding properties can be effectively studied using the model system of an atom embedded in a homogeneous electron gas. The only parameters of this model are the nuclear charge of the atom and the density of the electron gas. The screening cloud around the nucleus consists of localized bound states and delocalized scattering states which are solved self-consistently. Thus, the atom-in-jellium model is a good, simple reference system, which incorporates the essential features of the interaction between an atom with localized states and an environment with states of an extended nature. However, as for the real systems the electron gas can of course mimic only those with *sp*-type bonds. The relevant quantities describing the binding properties of an atom to an electronic environment can be extracted from the atom-in-jellium calculations as the parameters defined in the effective-medium theory (EMT).[17] The most important EMT parameters are the cohesive function $E_c(\bar{n})$ and the neutral sphere radius $s(\bar{n})$. They are calculated directly from the energy needed to immerse a free atom into the electron gas of density $\bar{n}$ and from the screening cloud around the nucleus in the electron gas. The minimum of $E_c(\bar{n})$ gives directly the EMT result for the cohesive energy of a simple metal, and in the case of, e.g., chemisorbed atoms or molecules, it gives the main contribution to the binding energy. Moreover, according to the EMT, $s(\bar{n})$ is the Wigner-Seitz radius of a simple metal and the curvature of $E_c(\bar{n})$ is related to the bulk modulus. In the case of molecules or chemisorbed atoms on solid surfaces the corresponding quantities are the bond lengths and the vibrational frequencies.

In addition to its simplicity, one of the benefits of studying the binding properties in the atom-in-jellium and/or the EMT scheme compared to systematic studies for solids and small molecules is that the present approach gives structure-independent information: there is no lattice structure or certain symmetry of the surrounding atoms. Therefore the investigation of the trends as a function of atomic number can be extended over all atoms, irrespective of, for example, the solid formed by the atoms in question being a metal or an insulator. Even the rare-gas solids can be treated in the formalism. Moreover, the binding properties are more specific to the atom than to a certain environment.

Also the EMT calculations using $E_c(\bar{n})$ obtained in the LDA indicate overbinding effects: For example, the chemisorption energy for O on metal surfaces is about 2–3 eV too large compared to the experimental values although the bond distance and the vibrational frequency perpendicular to the surface are predicted quite well.[18,19] In this work we calculate the EMT parameters using different approximations for exchange and correlation. Besides the LDA,[20] we solve the electron structures using the GGA and the SIC. Comparing the cohesive functions (especially their minima) obtained in different schemes parallel to the theoretical and experimental results for cohesive energies of solids and binding energies of diatomic molecules gives new insight about the origin of the errors in the LDA. We also show that the atom-in-jellium model is a relevant testing ground for approximations of the exchange-correlation functional. Moreover, the EMT parameters obtained are useful in the future applications of the EMT.

The organization of the present paper is as follows: In Sec. II we discuss the theoretical tools needed. First in Sec. II A the solution of the model problem of an atom embedded in electron gas is described in different approximations for electron exchange and correlation. Thereafter in Sec. II B the definitions of the EMT parameters are given. The results are presented and discussed in Sec. III. Section III A is devoted to the trends in the EMT parameters and their comparison with the first-principles results for metals. Section III B concerns the effects due to different exchange-correlation functionals on the EMT parameters. In Sec. III C the differences in the EMT binding energies between the LDA and the SIC are compared with the differences between theoretical LDA results and experimental results for cohesive energies of solids and for binding energies of diatomic molecules. For the possible applications in future, the EMT parameters calculated in the SIC are tabulated in Sec. III D. The corresponding parameters calculated in the LDA have al-

ready been published as tabulations elsewhere.[21] Finally, Sec. IV is a short summary.

II. THEORY

A. Atom in electron gas

In the present model problem[22,23] there are two parameters to be varied: the nuclear charge Z at the origin and the constant density $\bar{n}$ of the rigid positive background charge. The electron distribution $n(\mathbf{r})$ neutralizes these positive charges. The screening cloud consists of localized bound states and delocalized scattering states which are occupied from the energy zero up to the Fermi level $\varepsilon_F(\bar{n})$. In the density-functional theory the ground-state electron density $n(\mathbf{r})$ minimizes the total-energy functional $E[n]$, and in the specific case of an atom in electron gas $n(\mathbf{r})$ can be obtained by solving the (nonrelativistic) Kohn-Sham equations ($\hbar=e=m=1$)

$$[-\tfrac{1}{2}\nabla^2+v_{\text{eff}}(r)]\psi_i=\varepsilon_i\psi_i \ , \tag{1}$$

$$v_{\text{eff}}(r)=\frac{-Z}{r}+\int\frac{[n(r')-\bar{n}]}{|\mathbf{r}-\mathbf{r}'|}d\mathbf{r}'+\frac{\delta E_{\text{xc}}[n]}{\delta n} \ , \tag{2}$$

$$n(r)=\sum_i^{\text{occ}}|\psi_i(r)|^2=\sum_i^{\text{bound}}|\psi_i(r)|^2+\int_0^{\varepsilon_F}n(\varepsilon,r)d\varepsilon \tag{3}$$

self-consistently. Above $\delta E_{\text{xc}}[n]/\delta n$ is the functional derivative of the exchange-correlation functional $\delta E_{\text{xc}}[n]$ with respect to the electron density. In Eq. (3) $n(\varepsilon,r)$ is the local density of states. Equations (1)–(3) are presented in the spin-compensated formalism, because in electron gas the partly filled nl shells of free atoms either become completed or they merge in the continuum.

In the LDA the exchange-correlation functional is expressed as an integral over the product of the electron density $n(\mathbf{r})$ and exchange-correlation energy density $\varepsilon(n)$

$$E_{\text{xc}}[n]=\int n(\mathbf{r})\varepsilon_{\text{xc}}(n(\mathbf{r}))d\mathbf{r} \ . \tag{4}$$

The exchange-correlation energy density $\varepsilon_{\text{xc}}(n)$ is obtained from the results for the homogeneous electron gas.[20] In the GGA the exchange-correlation energy density depends also on the density gradient and the exchange-correlation energy can be written as[8]

$$E_{\text{xc}}[n]=\int n(\mathbf{r})\varepsilon_{\text{xc}}(n(\mathbf{r}),\nabla n(\mathbf{r}))d\mathbf{r} \ . \tag{5}$$

The functional derivative $\delta E_{\text{xc}}[n]/\delta n$ defines the exchange-correlation potential, which, in a given point, is a function of the electron density in that point only (LDA) or a function of both the local electron density and its gradient in the given point (GGA). Detailed expressions for the functionals used are given in Refs. 20 and 8.

The total energy $E^{\text{hom}}(\bar{n})$ of the system of an atom embedded in homogeneous electron gas relative to the energy of the electron gas is calculated from the total-energy functional $E[n]$ of the density-functional theory. The final practical form is

$$E^{\text{hom}}(\bar{n})=\sum_i^{\text{bound}}\varepsilon_i+\int_0^{\varepsilon_F}\varepsilon\Delta n(\varepsilon)d\varepsilon-\int_0^{\infty}dr\,4\pi r^2 v_{\text{eff}}(r)n(r)+\tfrac{1}{2}\int_0^{\infty}dr\,4\pi r^2[n(r)-\bar{n}][\phi(r)-Z/r]$$
$$+\int_0^{\infty}dr\,4\pi r^2\left[n(r)\varepsilon_{\text{xc}}\left[n(r),\frac{dn(r)}{dr}\right]-\bar{n}\varepsilon_{\text{xc}}(\bar{n})\right] \tag{6}$$

(in the LDA, of course, the exchange-correlation energy density ε_{xc} does not depend on the density gradient). Above, $\phi(r)$ is the Coulomb potential in the system and $\Delta n(\varepsilon)$ is the change in the density of states in the electron gas due to the "impurity" atom. The continuum part of the change in the density of states can be obtained from the energy derivatives of the scattering phase shifts defined in the present spherically symmetric potential,

$$\Delta n(\varepsilon)=\frac{2}{\pi}\sum_l\frac{\partial\delta_l}{\partial\varepsilon}(2l+1) \ . \tag{7}$$

The immersion energy $\Delta E^{\text{hom}}(\bar{n})$ of an atom into the electron gas of density $\bar{n}$ is defined as

$$\Delta E^{\text{hom}}(\bar{n})=E^{\text{hom}}(\bar{n})-E^{\text{atom}} \ , \tag{8}$$

where E^{atom} is the total energy for a free atom calculated using the same approximations for exchange and correlation as for $E^{\text{hom}}(\bar{n})$. As a matter of fact, the total energy (6) of an atom in jellium and the corresponding numerical code reduce to those for a free atom when the continuum electron states and the positive background are excluded. There is, however, the difference that the calculation for the atom in jellium is spin-compensated (i.e., there is no explicit spin dependence), while the free atoms with nonfilled shells have to be calculated using spin-dependent formalism. Both the LDA and the GGA have been generalized to the spin-dependent case. We denote the local spin-density approximation by the LSD.

In the density-functional formalism distinct particles are substituted by a continuous density distribution. Therefore a localized electron interacts with itself via the repulsive Coulomb interaction. In an exact density-functional formalism this interaction would be canceled exactly by the exchange-correlation functional similarly to the case of the Hartree-Fock approximation. However, in the LDA this cancellation, although numerically rather good, is not perfect. In order to correct for this unperfect cancellation in the LDA (or in the LSD), the self-interaction correction scheme[12] (SIC) introduces the total-energy functional in the form

$$E_{\mathrm{SIC}}[n_\uparrow(\mathbf{r}),n_\downarrow(\mathbf{r})]=E_{\mathrm{LSD}}[n_\uparrow(\mathbf{r}),n_\downarrow(\mathbf{r})]-\sum_{i\sigma}\delta_{i\sigma} \ . \tag{9}$$

Above, $E_{\mathrm{LSD}}[n_\uparrow(\mathbf{r}),n_\downarrow(\mathbf{r})]$ is the total-energy functional in the local spin-density approximation and it depends on the spin densities $n_\uparrow(\mathbf{r})$ and $n_\downarrow(\mathbf{r})$. ($E_{\mathrm{LSD}}[n_\uparrow(\mathbf{r}),n_\downarrow(\mathbf{r})]$ is a direct generalization of $E_{\mathrm{LDA}}[n(\mathbf{r})]$.) Furthermore,

$$\delta_{i\sigma}=\tfrac{1}{2}\int d\mathbf{r}\int d\mathbf{r}'\frac{n_{i\sigma}(\mathbf{r})n_{i\sigma}(\mathbf{r}')}{|\mathbf{r}-\mathbf{r}'|}+E_{\mathrm{xc}}^{\mathrm{LSD}}[n_{i\sigma},0] \ , \tag{10}$$

where $E_{\mathrm{xc}}^{\mathrm{LSD}}[n_{i\sigma},0]$ is the exchange-correlation energy functional in the LSD. The $i\sigma$ summation in (9) runs over all occupied localized states with spin index σ and orbital density $n_{i\sigma}(\mathbf{r})$.

Varying the SIC functional (11) with respect to the orbitals ψ_i one obtains a scheme similar to Eqs. (1)–(3). Now the effective potential depends on the orbital $i\sigma$,

$$v_{\mathrm{eff},i\sigma}(r)=v_{\mathrm{eff}}^{\mathrm{LDA}}(r)+v_{i\sigma}(r) \ , \tag{11}$$

where the orbital dependent part $v_{i\sigma}(r)$ arises from the correction (10) in the energy functional. Moreover, now one has to use a more general one-particle equation:

$$[-\tfrac{1}{2}\nabla^2+v_{\mathrm{eff},i\sigma}(r)]\psi_i=\sum_j\lambda_{ij}^\sigma\psi_j \ , \tag{12}$$

where the Lagrange parameters λ_{ij}^σ ensure that the orbitals are orthogonal against each other.

In the SIC calculations for the atoms in the electron gas the orbital-dependent corrections $v_{i\sigma}(r)$ are applied only to the bound localized states. In the case of delocalized states this correction vanishes due to the infinite extent of these states. The system of an atom in the electron gas is a simple test model for the SIC, because it is a one-center problem. In multicenter cases, of which a diatomic molecule is the simplest one, the SIC corrections depend on the choice of the orbitals: the orbitals can be chosen as localized around a given nucleus each, or as Bloch-type functions delocalized over the whole system. As in the case of free atoms[12,13] we find for atoms in jellium that the nonorthogonality between the bound states has only a small effect on the final results, and therefore the orthogonalization of the bound states is omitted in our calculations. But we also find that it is important to orthogonalize the scattering states against the bound states, especially if there are rather extended shallow bound states. Namely, in this case it is possible that although a shallow bound state exists for the self-interaction corrected potential, the potential for the scattering states, which is calculated without any self-interaction correction, does not bind that state. Without orthogonalization this leads to "double counting," because the state exists then also as a resonance at positive energies. The orthogonalization of the scattering state with the angular-momentum quantum number l and energy E is performed as

$$\psi_{l,E}^{\mathrm{orth}}(r)=\psi_{l,E}^{\mathrm{nonorth}}(r)-\left[\int_0^\infty\psi_{l,i}(r')\psi_{l,E}^{\mathrm{nonorth}}(r')4\pi r'^2dr'\right]\times\psi_{l,E}^{\mathrm{nonorth}}(r) \ , \tag{13}$$

where the summation runs over all bound states with the same l. The nonorthogonalized wave functions $\psi_{l,E}^{\mathrm{nonorth}}(r)$ are normalized so that beyond a certain cutoff radius R they smoothly join to the spherical waves with the radial part as

$$j_l(kr)\cos\delta_l(E)-n_l(kr)\sin\delta_l(E) \ , \tag{14}$$

where j_l and n_l are the spherical Bessel functions and $k=\sqrt{2E}$. We have calculated the immersion energies of atoms into the electron gas in the SIC using Eq. (8) with the SIC total-energy functionals for the atom in jellium as well as for the free atom.

B. The effective-medium theory

The effective-medium theory (EMT) is an approximative method for calculating the total energy of a system of interacting atoms.[17,24,25] It is fast enough in order that it can be applied in Monte Carlo or molecular-dynamics simulations. It is also important that the interatomic interactions are treated in the EMT in a transparent way, which gives new physical insight into the problem in question, and, e.g., for the trends seen it is easy to give a simple physical interpretation. The EMT is derived in the density-functional theory and the basic parameters needed in its applications can be calculated from the electronic structure for atoms in homogeneous electron gas. In this sense the EMT is thus an *ab initio* method.

The central concepts in the EMT are the neutral sphere radius $s(\bar{n})$ and the cohesive function $E_c(\bar{n})$. The radius $s(\bar{n})$ is calculated using the total electron density $n(r)$ around an atom in homogeneous electron gas with density $\bar{n}$, and requiring neutrality as

$$\int_0^{s(\bar{n})}n(r)4\pi r^2dr=Z \ . \tag{15}$$

Thus, the constant positive background charge is omitted above. The cohesive function $E_c(\bar{n})$ is then defined as

$$E_c(\bar{n})=\Delta E^{\mathrm{hom}}(\bar{n})-\alpha(\bar{n})\bar{n} \ , \tag{16}$$

where the function α is defined as

$$\alpha(\bar{n})=\int_0^{s(\bar{n})}dr\,4\pi r^2\phi(r) \ . \tag{17}$$

The last term in Eq. (16) cancels the Coulomb interaction of the positive background charge with the induced charge density inside the neutral sphere. This interaction is inherent in the immersion energy $\Delta E^{\mathrm{hom}}(\bar{n})$. Alternatively, this term can be considered as an attractive electrostatic interaction energy of the induced atomic charge with the homogeneous electron gas.

The immersion energies $\Delta E^{\mathrm{hom}}(\bar{n})$ and the cohesive energies $E_c(\bar{n})$ calculated in the LDA for a few atoms are shown in Figs. 1 and 2. Although not shown in Fig. 1, $\Delta E^{\mathrm{hom}}(\bar{n})$ should approach at the zero-density limit the electron affinity for the given atom, because the appropriate limit is a negative ion, if it exists. Moreover, in these cases the approach should take place with an infinite negative slope.[26] When the electron density increases $\Delta E^{\mathrm{hom}(\bar{n})}$ begins to rise monotonically after a minimum. This rise is due to the increase of the kinetic energy. The attractive electrostatic interaction $-\alpha(\bar{n})\bar{n}$ lowers the

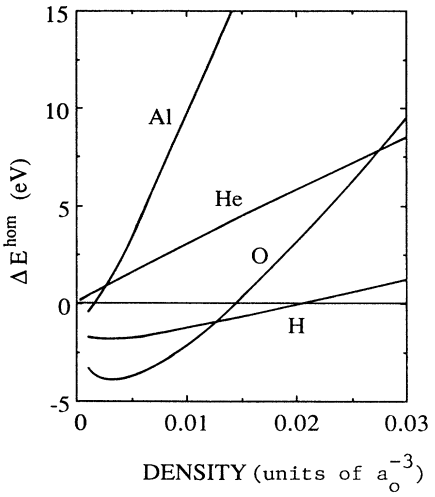

FIG. 1. Immersion energy ΔE^{hom} [Eq. (8)] as a function of electron-gas density for H, He, O, and Al. The electron structures are calculated within the LDA.

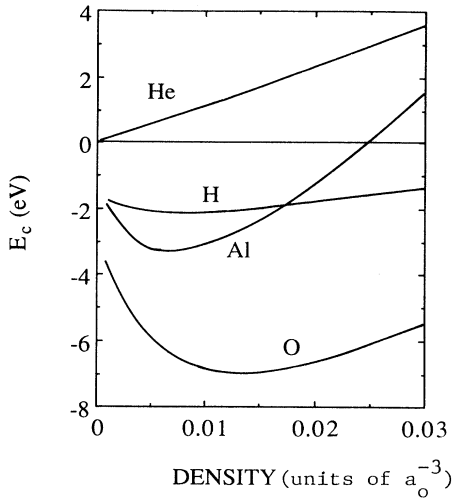

FIG. 2. Cohesive function E_c [Eq. (16)] as a function of electron-gas density for H, He, O, and Al. The electron structures are calculated within the LDA.

cohesive energy $E_c(\bar{n})$ relative to $\Delta E^{\text{hom}(\bar{n})}$. Moreover, the minimum of $E_c(\bar{n})$, which is at a higher density than that for $\Delta E^{\text{hom}(\bar{n})}$, results from the competition between the electrostatic interaction and the kinetic energy.

The minimum of E_c occurs at a certain density n_0, and the corresponding energy $E_c(n_0)$ gives in the EMT the cohesive energy of a simple metal. Moreover, because the background charge density $\bar{n}$ and the neutral sphere radius s obey a unique relation, there is a radius s_0 corresponding to n_0. In the EMT s_0 is the Wigner-Seitz radius of a simple metal. As a matter of fact, the relation between $\bar{n}$ and s follows rather accurately an exponential decay

$$\bar{n}(s)=n_0 e^{-\eta(s-s_0)} , \tag{18}$$

where η is a constant.

It is useful to parametrize $E_c(\bar{n})$ as a Taylor polynomial

$$E_c(\bar{n})=E_0+E_2(\bar{n}/n_0-1)^2+E_3(\bar{n}/n_0-1)^3 . \tag{19}$$

The third-order approximation is sufficient for most purposes but of course one cannot extrapolate it to high electron densities. For example, the parameter E_2 above gives the curvature of $E_c(\bar{n})$ around its minimum, and then the bulk modulus of a simple metal in the EMT can be expressed as

$$B=\frac{1}{12\pi s_0}\frac{d^2E_c}{ds^2}=\frac{1}{12\pi s_0}\eta^2 n_0^2\frac{d^2E_c}{d\bar{n}^2}=\frac{1}{12\pi s_0}\eta^2 E_2 . \tag{20}$$

If the EMT is applied to solids which are not simple metals, one has to introduce the so-called *one-electron energy* term, which takes into account, for example, the interatomic covalent interaction of the d electrons in a transition metal.[17] The EMT has been applied also for gas atoms chemisorbed on metal surfaces.[27,19] In these cases the chemisorption energy is determined mainly by the value of the minimum of the E_c curve. The equilibrium position and thus the bond length are approximately given by the fact that the adsorbed atom seeks out a region where the unperturbed electron density is close to n_0. The vibrational frequency perpendicular to the surface is mainly determined by the curvature of the E_c curve and the decay of the metal electron density near the surface.

Thus, according to the EMT the cohesive function $E_c(\bar{n})$ characterizes, in the case of a given atom, the chemical binding properties with a free-electron-like (or *sp*-electronlike) environment. The $E_c(\bar{n})$ curves and the corresponding EMT parameters $(s_0,n_0,\eta,E_c(n_0),\ldots)$ are properties of the atom itself, independent on the actual environment. One of the basic ideas in the EMT is that the properties of a system of interacting atoms can to a large extent be derived from the properties of the constituent atoms themselves. In this work we study the effects of different approximations on the cohesive function $E_c(\bar{n})$. The results obtained describe in a general sense the effects on the chemical-binding properties of the atoms, and therefore the conclusions drawn can be transferred to actual systems, too.

III. RESULTS AND DISCUSSION

A. Trends in the effective-medium-theory parameters

The self-consistent electron structures for atoms in a uniform electron gas and the corresponding immersion energies have been calculated within the LDA already previously for many cases. Popovic and Stott[28] reported on the first of this type calculation for H. The immersion energies for He and Li were published by Stott and Zaremba.[29] Puska, Nieminen, and Manninen[23] treated

the lightest atoms from H up to Ar, and Stott and Zaremba[22] published confirming results for atoms up to Ne. Results for the 3*d* series are reported in the paper by Jacobsen, Nørskov, and Puska.[17] We have redone the LDA calculations in this work. The numerical results from these calculations have been published elsewhere.[21] Small changes in the comparison with previous results are presumable due to the use of different exchange-correlation functionals and due to slightly different numerical approaches. The recalculation was necessary also because a complete set of the EMT parameters as a function of the atomic number does not exist previously.

We have plotted in Figs. 3 and 4 the behavior of the six EMT parameters as a function of the atomic number. The values are calculated in the LDA. The uppermost part of Fig. 3 shows the trend for the minima of the E_c curves. The magnitude $-E_c(n_0)$ increases in the beginning of the filling of the 2*p*, 3*p*, or 3*d* atomic levels and decreases when these levels are nearly full. In the middle of the 2*p* and 3*d* series there is a local minimum for $-E_c(n_0)$ and also a shoulder in the middle of the 3*p* series. These local minima and the shoulder reflect the

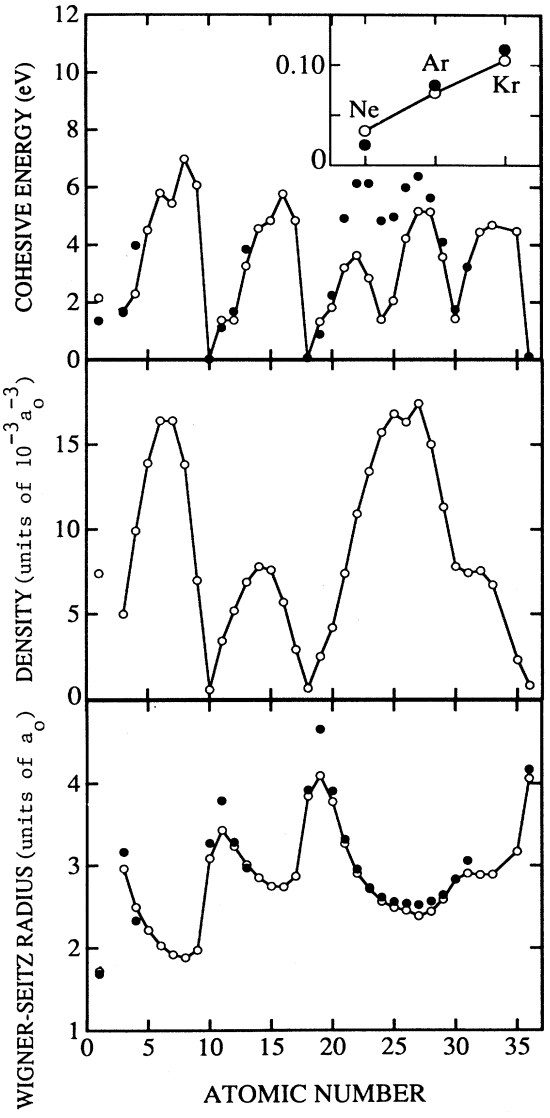

FIG. 3. EMT parameters calculated in the LDA for atoms from H to Kr (excluding He). The uppermost panel shows the magnitudes of the minimum values of the E_c functions: $|E_0| = |E_c(n_0)|$ (open circles). These values are compared with the first-principles theoretical cohesive energies for metals (Ref. 30) and with the experimental cohesive energies for rare gases (Ref. 35) (black circles). The middle panel gives the optimum densities n_0, which are the positions of the minima of the E_c functions. The lowest panel shows the radii s_0 of the neutral spheres corresponding to the minima of the E_c functions (open circles). The black circles give for metals and rare gases the Wigner-Seitz radii from first-principles theoretical calculations (Ref. 30) or from experiments (Ref. 35), respectively.

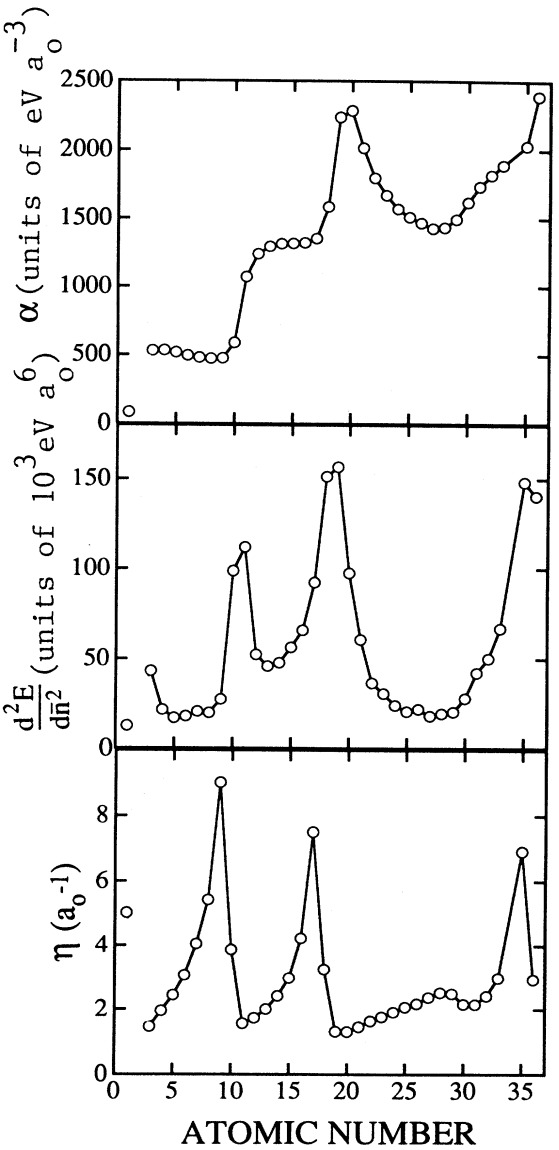

FIG. 4. EMT parameters calculated in the LDA for atoms from H to Kr (excluding He). Parameters α [Eq. (17)] and η [Eq. (18)] and the curvature $d^2E/d\bar{n}^2$ correspond to the minima of the E_c functions.

relatively large binding energies of the atoms which have half-filled shells and thus a large total spin momentum. The cohesive energies resulting from self-consistent KKR band-structure calculations by Moruzzi, Janak, and Williams[30] are shown in the uppermost panel of Fig. 3 for comparison. The first-principles results show similar rising trends in the beginning of each series and a minimum in the middle of the 3*d* series, as seen in $-E_c(n_0)$. The first-principles results for the metals in the middle of the 3*d* series are, however, much larger than the corresponding values of $-E_c(n_0)$. The difference signals the large contribution of the *d-d* interaction to the cohesive energy.[31] It is also noteworthy that the EMT result for Be is much smaller than that from the first-principles calculations.

The middle panel of Fig. 3 shows the position n_0 of the minimum of $E_c(\bar{n})$ as a function of the atomic number. The parameter n_0 shows a repeated, rather parabolic behavior with the maxima near the middle of the 2*p*, 3*p*, and 3*d* series. Thus the atoms with atomic shells approximately half-filled have a tendency to seek into regions with higher electron densities than the optimum densities for the atoms with nearly empty or filled open shells. This tendency has been shown, for example, to favor the formation of an icosahedral structure in the case of aluminum-transition-metal alloys.[32]

The neutral sphere radii s_0 show according to the lowest panel of Fig. 3 a different kind of trend than n_0: s_0 decreases as the open shell is filling in each of the three series and near the end of every series s_0 increases slightly. The Wigner-Seitz radii for metals from self-consistent band-structure calculations[30] are also shown in the lowest panel of Fig. 3. The s_0 values reproduce nicely all the trends and even the quantitative agreement is in most cases very good. However, in the case of alkali metals s_0 is clearly smaller than the values of the full calculations. The good agreement along the 3*d* series is of special importance, because the present calculations take into account the interaction of the atomic levels only with a *sp*-type environment. The good agreement is in accord with the conclusion of a pressure analysis that the lattice constant of the 3*d* transition metals is forbidden to shrink due to the increase of the *sp* partial pressure.[33] The inclusion of the *d-d* interaction into the EMT through the so-called one-electron-energy correction decreases slightly the neutral-sphere radii[17] and makes the agreement in the beginning of the 3*d* series slightly worse.

The curvature of the $E_c(\bar{n})$ function, i.e., $d^2E_c(\bar{n})/d\bar{n}^2$, and the EMT parameters η and α are given in Fig. 4 as a function of the atomic number. The curvature (as a function of $\bar{n}$) results mainly from the curvature of the change of the exchange-correlation energy when the atom is brought from vacuum into the electron gas. The contributions due to the changes of the kinetic and electrostatic energies are smaller. The curvature $d^2E_c(\bar{n})/d\bar{n}^2$ is approximately inversely proportional to the position n_0 of the minimum of the $E_c(\bar{n})$ function on the real axis. Therefore the curvature in the 2*p* and 3*p* series is at largest for the alkali metals and halogen atoms, the E_c curves of which rise nearly as steeply as the corresponding curves for rare-gas atoms.

The parameters η and α also show very interesting trends. The middle panel of Fig. 4 shows that η increases strongly in the 2*p* and 3*p* series towards the halogens F and Cl. According to Eq. (18) this means that in the case of halogens the neutral sphere radius s does not depend strongly on the background electron density $\bar{n}$. This behavior is a consequence of the large electronegativity of the halogen atoms: they pull in electrons strongly, resulting in a screening cloud resembling a *negative* ion, and therefore the radius at which the cloud *neutralizes* the nucleus is rather insensitive to the background electron density. The behavior of the parameter α, which is the integral of the Coulomb potential over the neutral sphere [Eq. (17)], is shown in the lowest panel of Fig. 4. It can be seen that α is nearly constant for the 2*p* series, slightly increasing along the 3*p* series, and has a clear decreasing trend towards the end of the 3*d* series. These trends result from two competing effects: the decrease of the neutral sphere radius s_0 within each series as a function of the atomic number tends to decrease the value of α and the simultaneous strengthening of the Coulomb potential tends to increase α. In the case of the 2*p* series, these two effects nearly cancel each other and the result is a nearly constant α. In the case of the 3*p* series s_0 does not decrease as fast as in the 2*p* series, because now there are the core *p* states, against which the outer (not bound) *p* states have to be orthogonal. As a result, α increases slightly along the 3*p* series. In the case of the 3*d* series there are no *d* states in the core, and s_0 as well as α can decrease rather strongly when the atomic number increases.

The density-functional calculations have led to a simple picture of metallic cohesion.[31,34] Especially the picture for the bulk modulus is very transparent. Namely, the bulk modulus for the actual metals with ions in a regular lattice can be identified as the bulk modulus of a free-electron gas with density equal to the interstitial electron density in the metal lattice. The ion cores (including the *d* electrons of the transition metals) act like rigid, nonoverlapping spheres, which limit the space available for the interstitial electron gas, but do not contribute in the bulk modulus. The differences in the bulk moduli between different metals have been shown to result mainly from the density dependence of the kinetic energy of the electron gas. However, the exchange-correlation energy plays an important role in determining the absolute value of the bulk modulus. Thus, it is no wonder that the EMT can reproduce quite well the first-principles results[30] for the bulk moduli of metals. This is shown in Fig. 5. In EMT the origins of the different trends in the bulk modulus can be further analyzed according to Eq. (20). Because n_0 and the curvature $d^2E_c(\bar{n})/d\bar{n}^2$ are roughly inversely proportional to each other, the factors, which mainly determine the behavior of the bulk modulus, are the proportionality to the square of η and to n_0 and the inverse proportionality to s_0. According to the middle panel of Fig. 3, η rises rapidly in the 2*p* and 3*p* series towards the halogen atoms. A large η [Eq. (18)] means that the background electron density

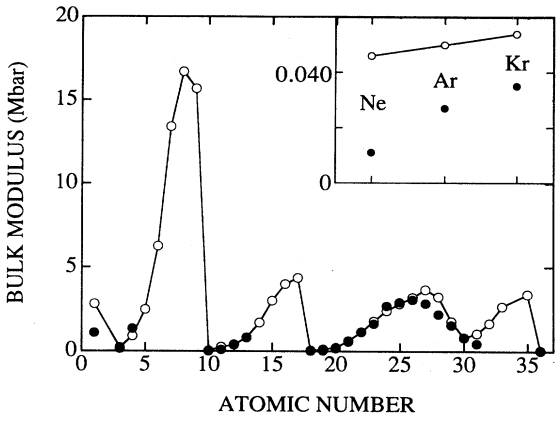

FIG. 5. Bulk moduli calculated in the LDA for atoms from H to Kr (excluding He). The EMT values (open circles) calculated according to Eq. (20) are compared with the first-principles theoretical results for metals (Ref. 30) and with the experimental bulk moduli for rare gases (Ref. 35) (black circles).

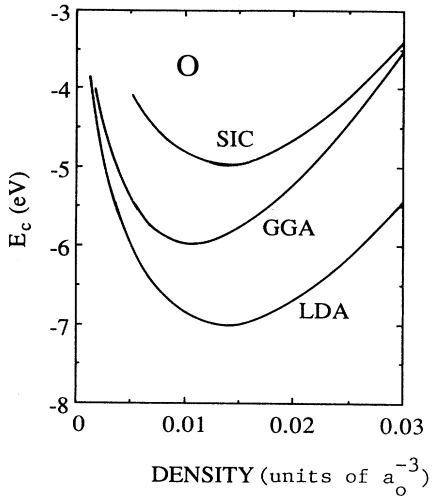

FIG. 6. Cohesive function E_c calculated for O within the LDA, GGA, and SIC.

changes rapidly when the volume changes. This raise of η explains the strong raise of the bulk modulus along the $2p$ and $3p$ series. In the $3d$ series the change of the η parameter is less dramatic, and the behavior of the bulk modulus reflects mainly the direct dependence of the background density n_0 on the atomic number.

We have found that the $E_c(\bar{n})$ functions calculated for the rare-gas atoms Ne, Ar, and Kr possess small but nevertheless clear minima at low-electron densities. In the case of He the $E_c(\bar{n})$ data do not show a minimum at least down to the lowest electron densities ($r_s = 12$) for which we were able to obtain self-consistent solutions. The ensuing EMT parameters for Ne, Ar, and Kr are collected in Table I and shown in Figs. 3–5, in which a comparison is made with experimental cohesive properties,[35] too. The theoretical and experimental cohesive energies and Wigner-Seitz radii are in good agreement. This is in accord with the Gordon-Kim model,[36] which is able to predict an attractive well in the interaction potential between two rare-gas atoms, and with the results by Lang[37] showing that the LDA is able to describe the physisorption of rare-gas atoms on metal surfaces. The experimental bulk moduli are, however, much smaller than the theoretical ones. This reflects the difficulties of the LDA at the low-electron density side of the $E_c(\bar{n})$ minimum: the energy rises too quickly as the electron density decreases. The situation is analogous to the case of the interaction of two screened point charges in electron gas. This interaction should have a long-range attractive $1/r^6$ tail.[38,39] We postpone the detailed discussion about rare-gas-atom interactions to a separate publication.

B. Comparison of the atom-in-jellium results in the LDA, SIC, and GGA

The immersion energies $\Delta E^{\text{hom}}(\bar{n})$ and the cohesive functions $E_c(\bar{n})$ in the LDA, GGA, and SIC are given for two typical cases, O and Al, in Figs. 6 and 7, respectively. The curves corresponding to the GGA and SIC lie above the LDA values although the difference between the LDA and SIC is hardly visible in the case of Al. Thus both the GGA and SIC reduce the overbinding in the LDA. The SIC curves are rather rigidly shifted relative to the LDA curves. The differences between the SIC and LDA values increase slightly towards the higher electron densities, but for the $E_c(\bar{n})$ functions the positions of the minima (n_0) as well as the curvatures near the minima are nearly the same for both approximations. On the other hand, the GGA curves are seen to approach the corresponding LDA curves at low densities but the difference increases strongly with increasing electron density. As a consequence, the minima of the $E_c(\bar{n})$ functions are at lower densities in the GGA and the curvature around the minima are larger than in the LDA. The neu-

TABLE I. The EMT parameters for rare gases Ne, Ar, and Kr. The parameters are calculated by solving the electronic structures for atoms in an electron gas in the LDA. For the definitions, see text.

Atom	s_0 (a_0)	n_0 (a_0^{-3})	η (a_0^{-1})	E_0 (eV)	E_2 (eV)	E_3 (eV)	α (eV a_0^3)
Ne	3.088	0.000 57	3.864	−0.034	0.016	−0.004	586.2
Ar	3.844	0.000 65	3.250	−0.072	0.032	−0.010	1585.
Kr	4.061	0.000 80	2.937	−0.105	0.045	−0.008	2391.

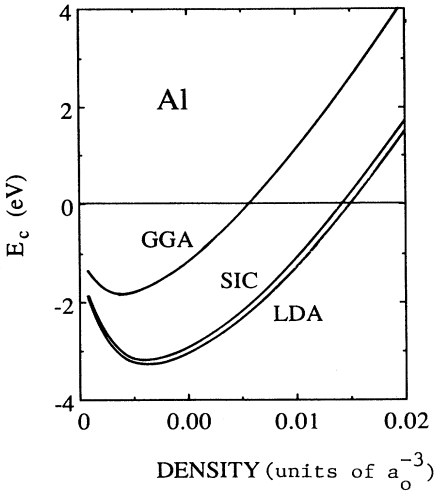

FIG. 7. Same as Fig. 6 but for Al.

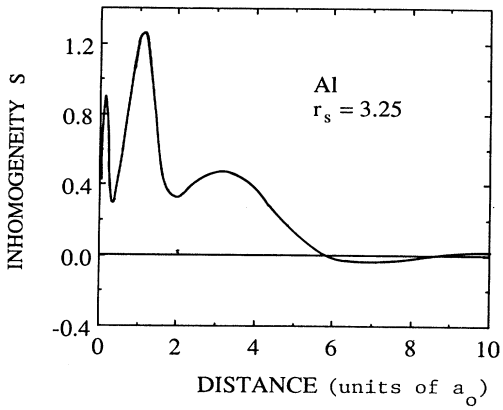

FIG. 8. Inhomogeneity parameter S [Eq. (21)] for an Al atom embedded in an electron gas with the density parameter $r_s = 3.25$.

tral sphere radii s_0 corresponding to n_0 are thus nearly the same for the LDA and SIC, whereas the GGA leads to a larger s_0. According to our calculations these trends between the different approximations are also valid for elements other than O and Al. The first conclusion on the basis of the $E_c(\bar{n})$ functions is that the SIC is able to heal the overbinding tendency of the LDA leaving unchanged the other cohesive properties, i.e., the bond lengths or Wigner-Seitz radii and the bulk moduli or the vibrational frequencies, which are well described in the LDA. Furthermore, the GGA seems to change all the cohesive properties, although, e.g., in the case of diatomic molecules only the GGA dissociation energies deviate strongly from the corresponding LDA results.[15] In the following we try to understand these trends by investigating the details of the electron densities.

In order to understand why the GGA does not work properly in the case of an atom in electron gas, we study the inhomogeneity parameter

$$S(r)=\frac{|\nabla n(r)|}{2n(r)k_F(n(r))} , \tag{21}$$

where k_F is the local Fermi wave vector

$$k_F(n)=(3\pi^2 n)^{1/3} . \tag{22}$$

The gradient expansion is formally valid if S is everywhere small compared to unity.[40] $S(r)$ is plotted for Al in jellium with $r_s=3.25$ in Fig. 8. We see that the inhomogeneity parameter is large outside the ion-core region ($r=1,\ldots,2$). This region contributes strongly to the energy differences (to the strength of the interaction of an atom with the environment) when the background electron density changes. The inhomogeneity and thus also the effect of the gradient correction increases towards higher background densities. Therefore also the $\Delta E^{\rm hom}(\bar{n})$ and $E_c(\bar{n})$ curves calculated in the LDA and GGA deviate from each other increasingly strongly with increasing jellium density. The behavior of the inhomogeneity parameter for an atom in jellium is very similar to that for metals.[41] Also in the case of jellium surfaces the GGA has been found to give unsatisfactory results for the surface energy, in which the contribution from the region of high inhomogeneity is also important.[42] On the other hand, the GGA gives very much improved results for free atoms,[42] in which case the large inhomogeneity at large distances does not matter, because the electron density and the contributions to energy terms far away from the nucleus are small. For free atoms the improvement in the GGA relative to the LDA is thus due to the better description of the atom core.

In order to understand the differences between the LDA and SIC results it is instructive to define a *relaxation charge* as the change of screening cloud of the nucleus when a free atom is brought into the electron gas,

$$\Delta n^{\rm rel}(r)=n(r)-\bar{n}-n^{\rm atom}(r) , \tag{23}$$

where $n(r)$ is the total electron density around the nucleus in electron gas, and $n^{\rm atom}(r)$ is the free-atom electron density. The relaxation charge is shown for O in jellium with $r_s=2.75$ in Fig. 9 and the corresponding plot

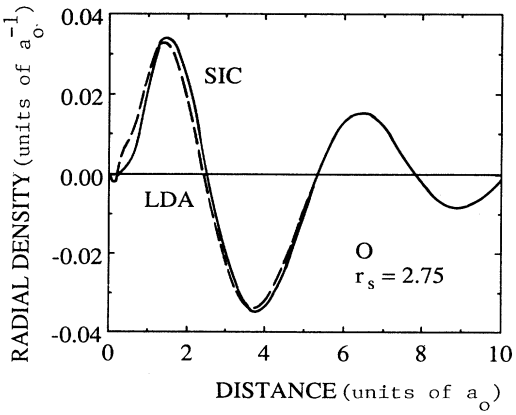

FIG. 9. Relaxation charge $\Delta n^{\rm rel}$ [Eq. (23)] for an O atom embedded in an electron gas with the density parameter $r_s=2.75$. The curves are obtained in the LDA (dashed line) and in the SIC (solid line).

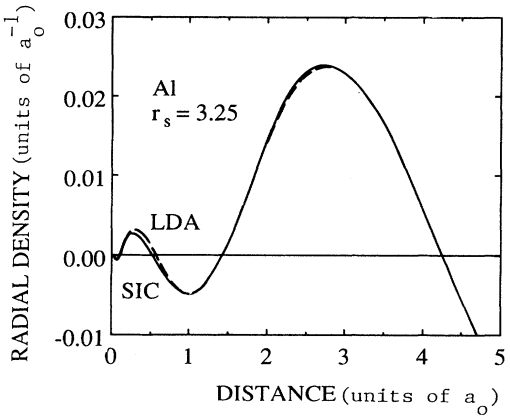

FIG. 10. Same as Fig. 9 but for an Al atom embedded in an electron gas with the density parameter $r_s = 3.25$.

for Al and $r_s = 3.25$ is in Fig. 10. (These r_s values correspond to the minima of the E_c functions.)

According to Fig. 9 for O, the relaxation near the nucleus is stronger in the LDA than in the SIC. This is a result of the self-interaction in the LDA: The self-interaction weakens the binding of electrons in the atomic levels and makes the states more extended. Therefore the relaxation is stronger in the LDA than in the SIC and the stronger relaxation means also larger energy lowering when the atom is brought from vacuum into electron gas. This explains why the ΔE^{hom} and E_c curves in the SIC are higher in energy than those in the LDA. It is interesting that the relaxation is stronger in the LDA than in the SIC although in the SIC O in jellium binds the $2p$ electrons while in the LDA it does not (oxygen in jellium is according to the SIC like an O^{2-} ion). In the case of the second-row elements from Be to N the differences in relaxation charges and energy functions are similar to those of O, but the $2p$ electrons are not bound. Thus the actual division to scattering states and to weakly bound localized states does not seem to be the critical parameter in the LDA-SIC comparison.

It can be noted from Fig. 9 that the large difference between the LDA and SIC relaxation densities is "screened out" at larger distances, which are important in determining the changes in ΔE^{hom} and E_c as a function of the background electron density. Therefore the forms of ΔE^{hom} and E_c are the same in the LDA and SIC; the SIC results are simply shifted to higher energies. As a matter of fact, if one draws the changes in the screening cloud between two different r_s values, the LDA and SIC results eventually coincide, meaning that the responses to the background density changes are similar in both systems. One can thus conclude that the SIC decreases the binding energy relative to the LDA because of the improved treatment of the electron density in the atom core region.

According to Fig. 7 the results calculated for Al in the LDA and SIC are nearly equal. The reason behind this can be clearly seen from Fig. 10, in which the relaxation charges [Eq. (23)] in the LDA and SIC are shown. The magnitude of the relaxation within the core region is small compared to the case of O in Fig. 9. This is due to the fact that Al has a compact core of the rare-gas Ne. Moreover, the curves corresponding to the LDA and SIC now lie close to each other reflecting the fact that the spatial extent of the deep-lying core states is moderately affected by the self-interaction. (Because the LDA raises rather rigidly the exchange-correlation potential compared to the potential in the exact density-functional theory, the atomic core densities are rather insensitive to the LDA although the energy eigenvalues are shifted remarkably upwards[43].)

C. Comparison of the atom-in-jellium results with theoretical and experimental dimer dissociation energies and bulk cohesive energies

According to the Sec. III A the simplest version of the EMT (ignoring the one-electron-energy and the atomic-spheres corrections) can describe those cohesive properties of solids, for which the d-d interaction is unimportant. In this section we demonstrate that the tendency of the LDA to lower the E_c curves relative to the corresponding SIC values is the same general overbinding deficit of the LDA, seen also in the case of dimer binding energies and the cohesive energies for bulk solids.

We have plotted in Fig. 11 the difference between the SIC and LDA values of the minimum of the E_c function as a function of the atomic number for elements from H to Cl. The differences of the dimer binding energies between the LDA calculations[15] and experiments[44] are also shown. Moreover, the deviations of the cohesive energies of solids calculated using the LDA (Ref. 30) from the experimental values[35] are added for the known cases. The trends are similar for all three differences: The LDA error rises as the atomic $2p$ level is filling and turns to descent at the halogen atom. The results deduced from the dimer dissociation energies and from the cohesive energies are even in a good quantitative agreement. The magnitudes of the atom-in-jellium results are of the same or-

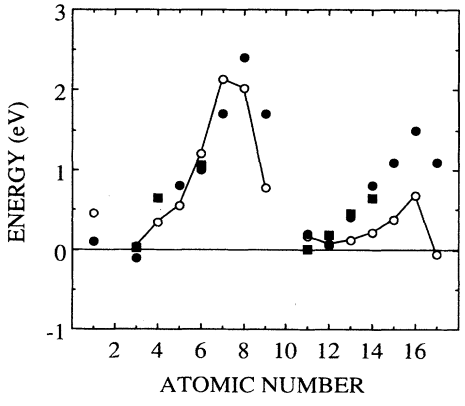

FIG. 11. Differences in the EMT cohesive energy $E_c(n_0)$ between the SIC and LDA (open circles) compared with the differences (Ref. 15) between the LDA and experimental dimer binding energies (black circles) and the differences between the first-principles theoretical LDA (Ref. 30) and experimental (Ref. 35) cohesive energies (black squares).

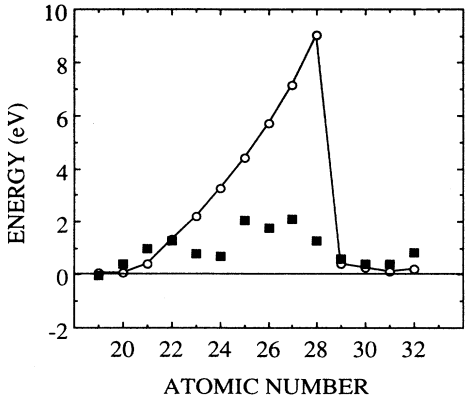

FIG. 12. Differences in the EMT cohesive energy $E_c(n_0)$ for $3d$ transition metals between the SIC and LDA (open circles) compared with the differences between the LDA between the first-principles theoretical LDA (Ref. 30) and experimental (Ref. 35) cohesive energies (black squares).

der as the results for dimers and bulk solids up to O, but after that the LDA-SIC differences in $E_c(n_0)$ are smaller than the latter two differences. The decrease of the SIC-LDA difference when going from the $2p$ series to the $3p$ series can be understood in the following natural way. Because the states filling the $3p$ shell have to be orthogonal against the inner $2p$ states, the relaxation charge [Eq. (23)] has to reside in the case of the $3p$ series further away from the nucleus than for the $2p$ series. Therefore in the $3p$ series the neutral sphere radii are larger, the energy change $E_c(n_0)$ smaller, and consequently also the difference in $E_c(n_0)$ between the SIC and LDA smaller than in the $2p$ series.

The differences between the SIC and LDA values for $E_c(n_0)$ in the $3d$ transition-metal series are shown in Fig. 12. In the figure the results are compared also with the differences between the experimental[35] and theoretical LDA (Ref. 30) cohesive energies. In the beginning and in the end of the series the differences in $E_c(n_0)$ and in cohesive energies are of the same order. In the middle of the series the LDA-SIC difference in $E_c(n_0)$ increases very strongly, whereas the LDA experiment difference in the cohesive energy shows a similar behavior as the cohesive energy itself. The reason for the increase of the LDA-SIC difference is the fact that in our model up to Ni the $3d$ electrons are not bound in the electron gas and therefore their self-interaction in jellium is not subtracted, which raises the immersion energy and $E_c(n_0)$ in the SIC. The $3d$ electrons form, however, a very narrow resonance and they are thus "quasilocalized." Therefore their treatment should be similar in a free atom and in an electron gas or in a solid.

D. EMT parameters in SIC

The EMT parameters calculated within the SIC are listed in Table II. The differences in the E_0 parameter or $E_c(n_0)$ between the SIC and the LDA have been discussed carefully above. Generally, the other parameters do not show dramatic changes when changing from the LDA to the SIC. The minimum of the $E_c(\bar{n})$ function, i.e., n_0, has a tendency to lie at lower densities in the SIC than in the LDA. The lowering is largest for H, Be, and F. The most dramatic difference happens in the case of the η parameter for F: The SIC value is nearly twice the LDA value. This difference reflects the enhancement of the negative-ion character in the SIC. The negative ion becomes more stable when the self-interaction is removed. Therefore the neutral sphere radius becomes less sensitive to the electron density of the environment and the η parameter increases. It is also interesting to note

TABLE II. Parameters for the effective-medium theory. The parameters are calculated by solving the electronic structures within the self-interaction correction scheme. For the definitions, see text.

Atom	s_0 (a_0)	n_0 (a_0^{-3})	η (a_0^{-1})	E_0 (eV)	E_2 (eV)	E_3 (eV)	α (eV a_0^3)
H	1.775	0.0055	5.279	−1.674	0.279	−0.093	75.6
Li	2.995	0.0048	1.451	−1.653	0.494	−0.286	535.4
Be	2.633	0.0076	1.928	−1.955	0.913	−0.580	560.4
B	2.259	0.0125	2.449	−3.905	1.472	−0.806	522.6
C	2.032	0.0164	3.053	−4.591	1.996	−0.674	495.6
N	1.919	0.0166	3.867	−3.257	2.357	−1.019	478.9
O	1.879	0.0138	6.083	−4.947	1.763	−0.513	467.3
F	1.935	0.0054	15.572	−5.281	0.583	−0.295	437.2
Na	3.468	0.0033	1.496	−1.206	0.382	0.060	1082.8
Mg	3.300	0.0047	1.722	−1.285	0.652	−0.219	1250.0
Al	3.059	0.0063	1.997	−3.165	1.136	−0.423	1301.1
Si	2.854	0.0078	2.404	−4.379	1.426	−0.761	1314.2
P	2.745	0.0077	3.035	−4.448	1.496	−0.580	1323.0
S	2.693	0.0071	3.992	−5.114	1.733	−0.523	1354.7
Cl	2.856	0.0029	7.760	−4.884	0.343	−0.090	1345.3
K	4.029	0.0027	1.280	−1.255	0.672	−0.324	2229.7
Ca	3.708	0.0044	1.266	−1.769	0.714	−0.076	2247.0

that in the case of the next halogen, Cl, the differences between the LDA and SIC values are very small. This results from the fact that the $3p$ states have to be orthogonal against the $2p$ states and therefore the self-interaction has less dramatic effects.

IV. CONCLUSIONS

In the present work we have demonstrated that the binding properties of atoms can be systematically investigated with the atom-in-jellium–effective-medium approach. This is true as long as the interactions with an sp-type electronic environment are considered. We have also demonstrated that the approach can be used for studying the effects of different approximations for electron exchange and correlation. For these studies the atom-in-jellium model constitutes a simple but useful model, which gives (lattice) structure-independent information about the interaction between the states localized at the atom and the delocalized scattering states.

According to our results the overbinding tendency of the LDA in the sp-bonded systems is reduced in the GGA and in the SIC. However, the deficiency found for the GGA is that it changes the EMT parameters related to bond distances and vibration frequencies considerably from those obtained in the LDA, which predicts these properties in a fair agreement with experiments. When the EMT parameters are calculated in the SIC only the strength of the binding is reduced remarkably, whereas the other parameters remain close to their LDA values. The differences between the LDA and the SIC can be understood by comparing the relaxations of electron densities when a free atom is embedded in an electron gas. Due to the self-interaction the electron structure in the LDA is not so compact as in the SIC and therefore the electron density near the nucleus relaxes more strongly in the LDA than in the SIC. This tendency is especially strong for atoms with a partially filled $2p$ shell. The stronger relaxation results in a larger energy change and binding energy in the LDA compared to the SIC. The differences in the relaxation charges are diminished at larger distances and the responses to the changes of the background electron-gas densities are similar in the LDA and SIC. This explains why the other EMT parameters than the bottom of the binding energy curve are similar in the LDA and SIC.

[1]R. O. Jones and O. Gunnarsson, Rev. Mod. Phys. **61**, 689 (1989).

[2]*Density Functional Methods in Physics,* Vol. 123 of *NATO Advanced Study Institute, Series B: Physics,* edited by R. M. Dreizler and J. da Providência, (Plenum, New York, 1985).

[3]*Theory of the Inhomogeneous Electron Gas,* edited by S. Lundqvist and N. H. March (Plenum, New York, 1983).

[4]O. Gunnarsson and B. I. Lundqvist, Phys. Rev. B **13**, 4274 (1976).

[5]J. P. Perdew and M. Levy, Phys. Rev. Lett. **51**, 1884 (1984).

[6]L. J. Sham and M. Schlüter, Phys. Rev. Lett. **51**, 1888 (1984).

[7]J. Harris and R. O. Jones, J. Chem. Phys. **68**, 3316 (1978); **70**, 830 (1979); R. O. Jones, *ibid.* **71**, 1300 (1979).

[8]J. P. Perdew and Wang Yue, Phys. Rev. B **33**, 8800 (1986); J. P. Perdew, *ibid.* **33**, 8822 (1986).

[9]O. Gunnarsson, M. Jonson, and B. I. Lundqvist, Phys. Lett. **59A**, 177 (1976).

[10]O. Gunnarsson, M. Jonson, and B. I. Lundqvist, Solid State Commun. **24**, 765 (1977).

[11]D. C. Langreth and M. J. Mehl, Phys. Rev. Lett. **47**, 446 (1981); Phys. Rev. B **28**, 1809 (1983).

[12]J. P. Perdew and A. Zunger, Phys. Rev. B **23**, 5048 (1981).

[13]O. Gunnarsson and R. O. Jones, Solid State Commun. **37**, 249 (1981).

[14]O. Gunnarsson and R. O. Jones, Phys. Rev. B **31**, 7588 (1985).

[15]A. D. Becke, in *The Challenge of d and f Electrons,* edited by D. R. Salahub and M. C. Zerner, ACS Symposium Series No. 394 (American Chemical Society, Washington, D.C., 1989), p. 165.

[16]F. W. Kutzler and G. S. Painter, Phys. Rev. Lett. **59**, 1285 (1987).

[17]K. W. Jacobsen, J. K. Nørskov, and M. J. Puska, Phys. Rev. B **35**, 7423 (1987).

[18]B. Chakraborty, S. Holloway, and J. K. Nørskov, Surf. Sci. **152/153**, 660 (1985).

[19]U. Yxklinten, in *Many-Atom Interactions in Solids,* edited by R. M. Nieminen, M. J. Puska, and M. Manninen, Springer Proceedings in Physics Vol. 48 (Springer, Berlin, 1990), p. 314.

[20]We use the local exchange-correlation functional based on the results by D. M. Ceperley and B. J. Alder, Phys. Rev. Lett. **45**, 566 (1980), and the parametrized form given in Ref. 12.

[21]M. J. Puska, in *Many-Atom Interactions in Solids,* edited by R. M. Nieminen, M. J. Puska, and M. Manninen, Springer Proceedings in Physics Vol. 48 (Springer, Berlin, 1990), p. 134.

[22]M. J. Stott and E. Zaremba, Can. J. Phys. **60**, 1145 (1982).

[23]M. J. Puska, R. M. Nieminen, and M. Manninen, Phys. Rev. B **24**, 3037 (1981).

[24]K. W. Jacobsen, Commun. Condensed Matter Phys. **14**, 129 (1988).

[25]K. W. Jacobsen, in *Many-Atom Interactions in Solids,* edited by R. M. Nieminen, M. J. Puska, and M. Manninen, Springer Proceedings in Physics Vol. 48 (Springer, Berlin, 1990), p. 34.

[26]M. J. Stott and E. Zaremba, Phys. Rev. B **22**, 1564 (1980).

[27]K. W. Jacobsen and J. K. Nørskov, Phys. Rev. Lett. **59**, 2764 (1987).

[28]Z. D. Popovic and M. J. Stott, Phys. Rev. Lett. **33**, 1164 (1974).

[29]M. J. Stott and E. Zaremba, Solid State Commun. **32**, 1297 (1979).

[30]The cohesive energies calculated in the LDA are from V. L. Moruzzi, J. F. Janak, and A. R. Williams, *Calculated Electronic Properties of Metals* (Pergamon, New York, 1978) (metals); A. K. McMahan, Phys. Rev. B **30**, 5385 (1984) (C and Si); M. S. Hybertsen and S. G. Louie, *ibid.* B **30**, 5777 (1984) (Ge).

[31]A. R. Williams and U. von Barth, in Ref. 3, p. 189.

[32]A. C. Redfield and A. Zangwill, Phys. Rev. Lett. **58**, 2322 (1987); A. Zangwill and A. C. Redfield, J. Phys. F **18**, 1

(1988).
[33]A. R. Williams, C. D. Gelatt, and J. F. Janak, in *Theory of Alloy Phase Formation,* edited by L. H. Bennett, Conference Proceedings of the Metallurgigal Society of AIME (1979).
[34]O. K. Andersen, O. Jepsen, and D. Glötzel, in *Highlights of Condensed-Matter Theory,* edited by F. Bassani, F. Fumi and M. P. Tosi (North-Holland, Amsterdam, 1985).
[35]See C. Kittel, *Introduction to Solid State Physics* (Wiley, New York, 1976).
[36]R. G. Gordon and Y. S. Kim, J. Chem. Phys. **56**, 3122 (1972).
[37]N. D. Lang, Phys. Rev. Lett. **46**, 842 (1981).
[38]A. C. Maggs and N. W. Ashcroft, Phys. Rev. Lett. **59**, 113 (1987).
[39]D. C. Langreth and S. H. Vosko, Phys. Rev. Lett. **59**, 497 (1987).
[40]P. Hohenberg and W. Kohn, Phys. Rev. **136**, B864 (1964).
[41]O. Gunnarsson, M. Jonson, and B. I. Lundqvist, Phys. Rev. B **20**, 3136 (1979).
[42]J. P. Perdew, M. K. Harbola, and V. Sahni, in *Condensed Matter Theory,* edited by J. Arponen, R. F. Bishop, and M. Manninen, (Plenum, New York, 1988), Vol. 3.
[43]C.-O. Almbladh and A. C. Pedroza, Phys. Rev. A **29**, 2322 (1984).
[44]K. P. Huber and G. Herzberg, *Molecular Spectra and Molecular Structure IV: Constants of Diatomic Molecules* (Van Nostrand Reinhold, New York, 1979).